Backwards Step Numerical Simulation analysis

Author
Rik Williamson

MEC320 CFD

Department of Mechanical Engineering

May 2023

1 Computational domain and Discretisation process

1.1 Computational Domain

Dimension/Condition	Description	Value
U_{in}	Inlet velocity	44.2 m/s
$U_{in,b}$	Boundary Inlet Velocity	41.8 m/s
H	Step height	1.27 cm
x_{bl}	Boundary layer thickness	1.9 cm
L_{inlet}	Inlet Length	1.6 m
x_h	Flow domain height	10.16 cm

Table 1: Table showing the dimensions and conditions for the computational domain of the CFD model

The computational domain of the model is set by the boundary layer thickness at 4H before the step, inlet velocity, pressure and temperature of the experiment performed by Driver and Seegmiller [1]. A computational domain was constructed to meet these restrictions and therefore allow for useful comparison with the results obtained from this experiment. This was performed by iteratively altering the inlet length and observing where the velocity at 4H before the step reaches its asymptomatic value using a velocity profile plot. The effect of outlet length was quantified using a similar approach, where the length was altered and the resulting flow behaviour analysed. From these studies it was concluded that an inlet of 1600mm resulted in the required boundary layer thickness of 1.9 cm and the velocity of 44.2 m/s at 4H behind the step. To achieve this, the boundary condition inlet velocity also had to be altered to 41.8 m/s to achieve 44.2 m/s at 4H behind the step. The study also revealed that an outlet of 400mm was optimal, as beyond this point there is no significant variation in reattachment point or flow behaviour in the recirculating zone. Outlet pressure was set to that of atmospheric conditions to adhere to the conditions (101,325 Pa) used in the paper [1].

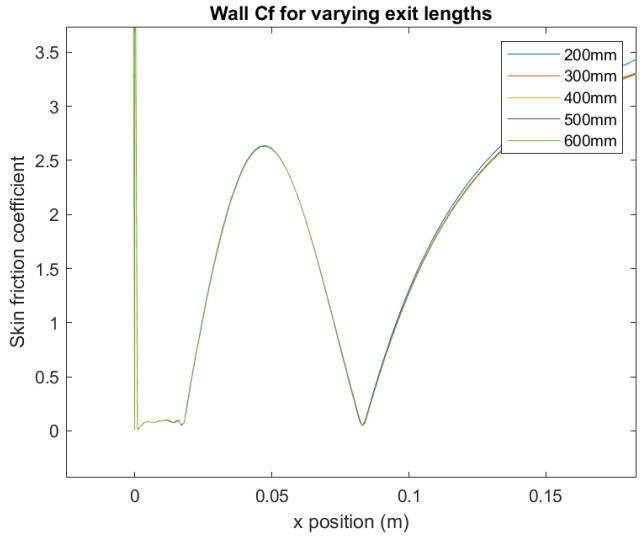

Figure 1: Graph showing the affect of exit length on the reattachment point

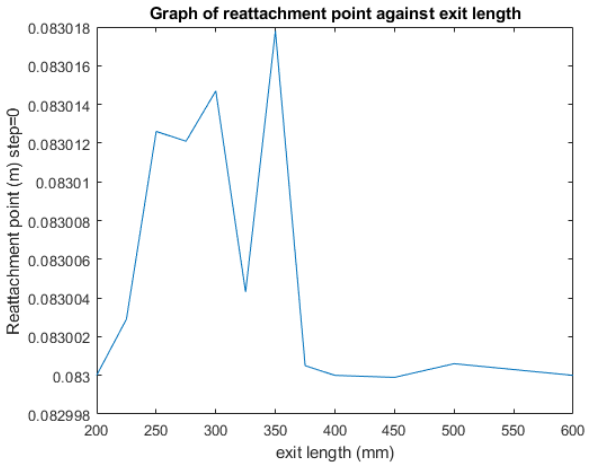

Figure 2: Graph showing the reattachment point ($c_f = 0$) for varying exit lengths

1.2 Meshing Strategy

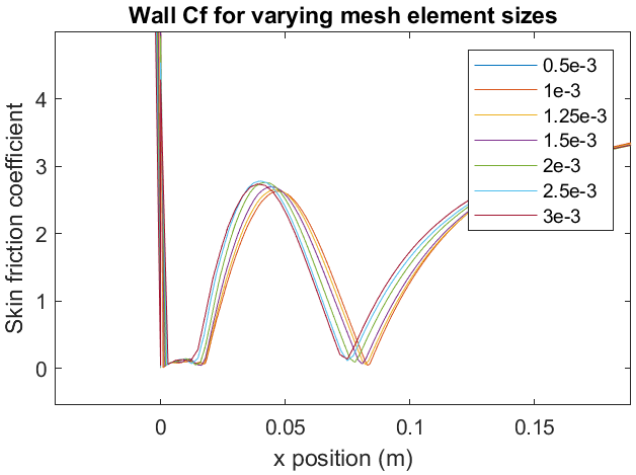

Figure 3: Graph showing wall Skin friction in the re-circulation region for varying element sizes

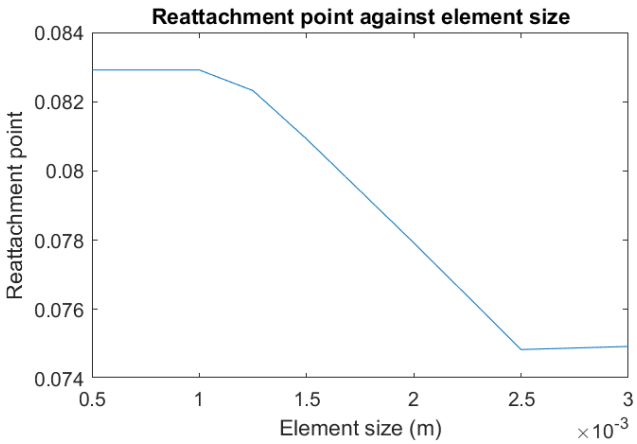

Figure 4: Graph showing the reattachment point ($c_f = 0$) for varying element sizes

Various meshing strategies were attempted with the goal to reach mesh independence and keep the y^+ value at the wall in the area of interest below 1 to allow for direct wall resolving with the chosen k-omega SST model. Splitting of the geometry at the step was performed in order to create regular elements without skewness and a small aspect ratio, especially at the step itself due to the sensitivity described in the Driver and Seegmiller paper [1]. Edge bias factors were then added to refine the mesh in the area of interest without adding unnecessary computation, however large aspect ratios and skewness near the step area due to the expanding domain necessitated use of an altered method. As a result, splitting of the bodies at a geometry level was performed and 'shared topology' enforced at the interfaces between the bodies to avoid discontinuity. Although this resulted in an even and regular mesh, initial simulations showed y^+ values orders of magnitude above 1, which resulted in wall modelling instead of direct resolving. To rectify this, a larger bias factor was imposed, refining the mesh near the wall further. However, to achieve y^+ below 1, a very large bias factor was required which resulted in low element quality in the area leading to the step and within. To solve this, an inflation layer was added to the ball boundary, allowing for definition of the first layer thickness and thus more fine control over y^+. This produced its own problems due to the inflation layer 'pinching' at the corner of the step at the interface between the bodies. The decision was therefore made to revert to a single body and face, which resulted in the intended inflation behaviour around the step corner, however was incompatible with edge bias for element sizing control. Instead, simple global element size control was implemented, allowing for the inflation layer to work as intended as well as insuring square, low aspect ratio and continuous elements throughout the mesh. Although this sacrifices computational efficiency, it allows for incremental and reliable varying of the mesh density for independence studies, without time consuming bias factor sizing changes between mesh densities.

During choice of inflation layer attributes, it was observed that convergence was heavily dependent upon the first layer size, growth rate and number of inflation layers. Gradual growth in the inflation layers and a minimum of 3 layers were required in this case for the solution to

converge. Without this, its suspected that the large gap between the first layer and subsequent node cause an error which propagates throughout the mesh.

1.3 Discretisation

The program used for this report, ANSYS Fluent, uses a Finite Volume Method. This Integrates over the RANS PDE over control volumes created during the meshing process, resulting in a system of algebraic equations which can be solved iteratively. Convection schemes are used to approximate points within the CV (control volume) and at the CV faces using known nodal values. In this model, the Second-order Upwind scheme was used which interpolates values using a straight line fit between two upstream nodal values. The direction of these upwind points depends upon the direction of mass fluxes through the relevant east of west faces. An advantage of this scheme over a First Order Upwind scheme is that it is second order accurate which reduces the numerical error proportionally to Δx^2. This reduces the need for a very fine mesh, resulting in quicker convergence and lower computing overhead. However due to it being unbounded, special consideration must be taken to ensure mesh refinement in areas of steep gradients where it can produce under and overshoots. This was observed during creation of the inflation layer in the mesh, where it's suspected that the large gradient from the wall to the surrounding mesh resulted in under/over shoot and therefore an unstable solution. The purpose of refining the mesh is to ensure mesh independence of the solution, eliminating it as a source of error.

2 Solution process

A pressure-based solver was chosen due to the assumption of incompressible flow being applicable due to the low Mach number. A coupling scheme had to be chosen due to the lack of explicit coupling between pressure and momentum in the continuity equation. A segregated algorithm could have been used, which guesses a pressure field, solves the momentum field then corrects pressure and velocity until the continuity equation is satisfied. Various segregated algorithms exist, with different correction methods; the more complex these algorithms, the more accurate the solution but the higher the computational expense. The Coupled algorithm, however, solves the conservation equations simultaneously at every iteration for velocity and pressure. Although this requires more memory due to the storage of large systems of equations, convergence is usually reached quicker. For this problem, a coupled scheme was chosen due to superior performance for steady-state problems [2]. The k-omega SST turbulence model was chosen as it uses a k-omega model in the inner boundary layer and k-epsilon near the wall which excels for flows with separation and adverse pressure gradients. For this particular flow scenario, near step wall flow was found to be crucial, therefore this model helps to capture turbulence characteristics more reliably. The model also excels with capturing flow transition phenomena from laminar to turbulent which is particularly important in the area after the step where the flow undergoes significant changes. Both turbulent eddy viscosity and turbulent shear stress transport are modelled with this approach, resulting in more accurate representation of the anisotropic flow behaviour present in the recirculating region due to complex vortical structures.

Both residual values and monitoring points are used in combination to determine whether

convergence has been achieved. Residuals measure the difference (error) between two sides of the conservation equations. These values are usually scaled relative to the local value of ϕ, allowing for comparison of all residuals on a single graph. In fluent, normalisation is also performed, where the relative error (R^{ϕ}) at the current iteration is divided by R^{ϕ} after a small number of iterations (in fluent, 5).

Monitoring points show the value of a particular flow parameter at each solve iteration. Choice of flow parameter is important, as an insensitive parameter such as freestream velocity in the inlet region of pipe flow, will converge quickly and thus not be representative of convergence of the solution for more sensitive flow characteristics. For this study, monitoring points were added at; the intended boundary layer height (1.9 cm) 4H before the step, freestream 4H before the step, after the step and in the recirculation region. Within these locations, static pressure, velocity magnitude minimum, maximum and Turbulent kinetic energy were sampled. Locations for these points were chosen after observing contour plots of the parameters listed above, with areas of large gradients or variance being considered. The Driver and Seegmiller[1] paper was also consulted to identify areas of sensitivity. Before experimentation, it was suspected that the most sensitive, easily retrievable parameter would be minimum or maximum velocity/static pressure either in the recirculation zone, or just after the step in the boundary. However, it was discovered that velocity magnitude at the boundary layer height 4H before the step required a larger number of iterations to converge than all other parameters tested.

3 Validation of results

3.1 Qualitative analysis

From visual inspection of figure 7, it can be seen that velocity increases above that of freestream (44.2 m/s) before the step. This was also observed during alteration of the inlet length to ensure boundary layer thickness continuity between the experimental results; where velocity 'overshot' after the boundary layer to above the freestream value. This is due to the expanding domain causing an area of low pressure (See figure 8), accelerating the upstream flow. Figure 7 also shows the characteristic dividing stream line, zero velocity magnitude at the reattachment point, the recirculating region and separation at the bottom step, with velocity reaching near zero in those areas. Pressure also follows the expected behaviour, with a large drop after the step and in the recirculating region and return to atmospheric conditions after reattachment.

3.2 Quantitative analysis

Figures 9 and 10 show agreement between the experimental and simulation results. Skin friction coefficient from the simulation was smaller than the experimental results, with the 'dip' in the recirculation zone being more pronounced. In the area near reattachment (≈ 0.083) the two results are very similar, indicating accuracy of the model for this area in particular. Agreement is also seen in the separation zone below the step, however this is suspected to be due to stagnant flow. Despite this, the similarity validates further that the model displays experimental flow characteristics. It must also be stated that Driver and Seegmiller's paper [1] states uncertainties in the range of $\pm 8\%$ to $\pm 15\%$, which implies that exact adherence doesn't necessarily imply model accuracy. The reattachment point found from the simulations and $Cf \approx 0$ is very close to that found from Driver and Seegmiller's paper. Interpolating from figure 2 [1], the reattachment

point found is $\approx 6.3x/H$ which results in an x position of 8 cm; a 3.6% change from the 8.3cm found from the model used in this report. This is closer than the most accurate model found by Driver and Seegmiller ($\approx 9\%$ difference), however this is not surpising given the advancements in CFD models and computing power. Differences between the model and experiment could be due to assumptions made from turbulence modelling, measurement/instrumentation errors or small differences in boundary conditions.

3.3 Sensitivity report

A sensitivity analysis was performed where values of the inlet velocity and step height were changed by $\approx 10\%$ respectively and the resulting wall skin friction and reattachment points observed. As seen in figure 11, changing the inlet velocity had a relatively small effect on the reattachment point; an inlet velocity change from 41.8 m/s to 32 m/s (23%) yielded only a $\approx 1.2\%$ increase in reattachment point. From this, it can be concluded that errors in choice of inlet velocity in the simulation would have resulted in a relatively small error in prediction of the reattachment point. Step size however, had a larger effect on reattachment as seen in figures 13 and 14 where a 6.3% change in step size (1.27cm to 1.35cm) resulted in an increase in reattachment of 7%. A similar change is observed with a decrease in step height, showing an almost linear relationship (see figure 14), although it cannot be assumed to be completely linear due to the limited data points available and complex flow behaviour. Inlet velocity changes did affect other regions of the flow, however. As can be seen in figure 12, a macro view shows proportionally larger skin friction coefficients in the recirculation and after reattachment, where Cf diverges. A similar phenomenon is observed before the step where larger inlet velocities result in larger skin friction coefficients which is due to the increased velocities resulting in increased shear stresses at the wall. It is theorised that higher reattachment sensitivity to step height changes is due to invariability of the dividing streamline with respect to step height itself. This causes reattachment to change proportionally with the geometric extension of the conserved streamline. Interestingly, step height changes did not alter the magnitude of Cf significantly, instead shifting the curve in the x direction (see figure 13). This corroborates the previous theory as the curve in this area is seen to scale proportionally in the x direction.

WORD COUNT: 2066

References

[1] D. M. Driver and H. L. Seegmiller, "Features of a reattaching turbulent shear layer in divergent channelflow," *AIAA Journal*, vol. 23, pp. 163–171, Feb. 1985. Publisher: American Institute of Aeronautics and Astronautics.

[2] "ANSYS FLUENT 12.0 User's Guide - 26.3.1 Choosing the Pressure-Velocity Coupling Method."

4 Figures

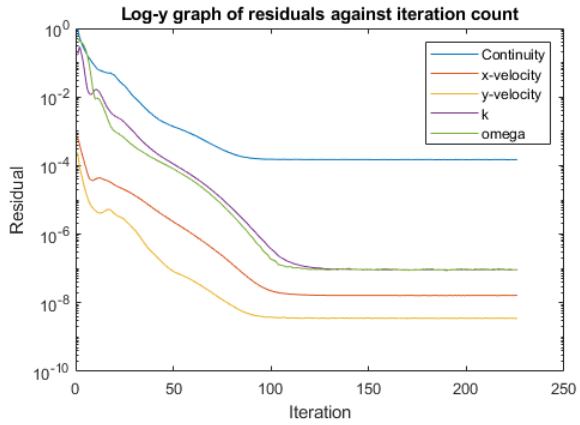

Figure 5: Graph showing normalised residuals with solution iterations

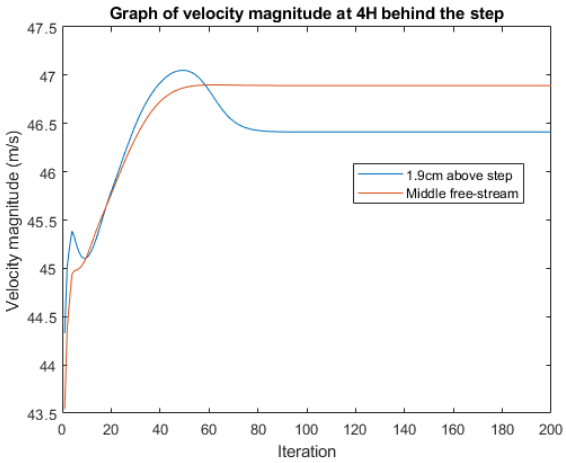

Figure 6: Graph showing freestream and boundary layer thickness velocities with solution iterations

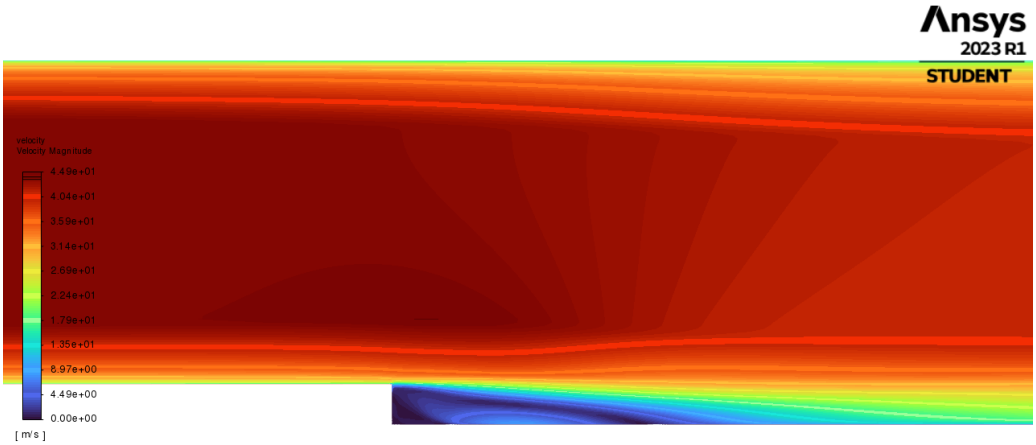

Figure 7: Graph showing normalised residuals with solution iterations

Figure 8: Graph showing freestream and boundary layer thickness velocities with solution iterations

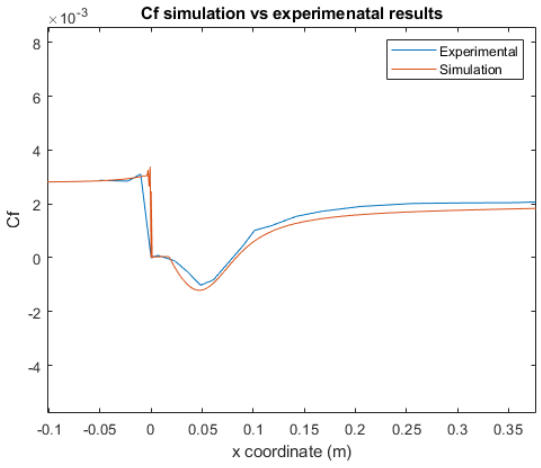

Figure 9: Graph showing comparison of Experimental and Simulation results for Cf

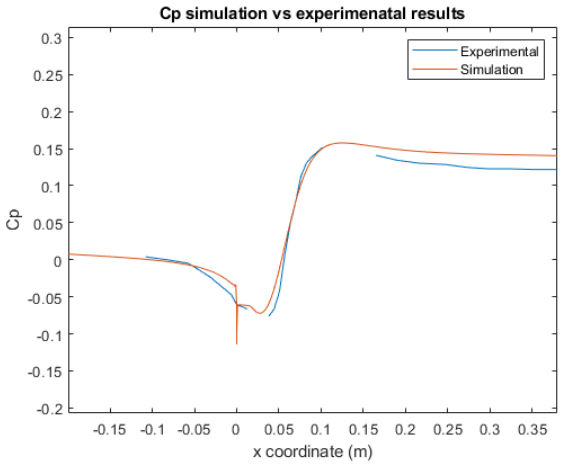

Figure 10: Graph showing comparison of Experimental and Simulation results for Cp

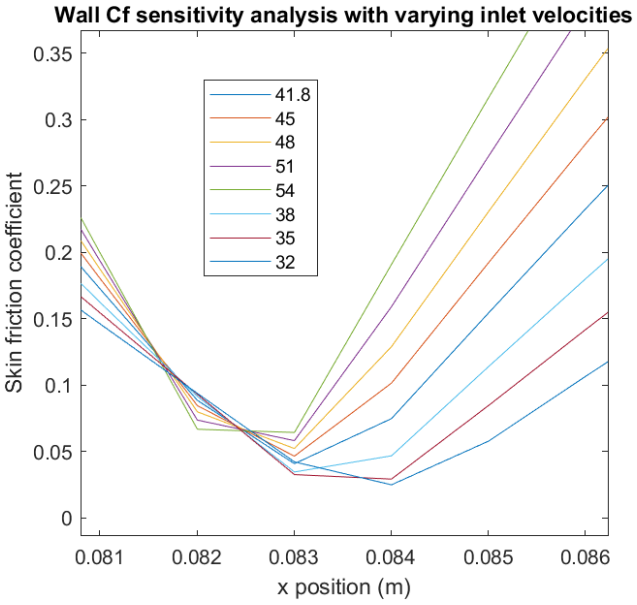

Figure 11: Wall Cf sensitivity analysis with varying inlet velocities

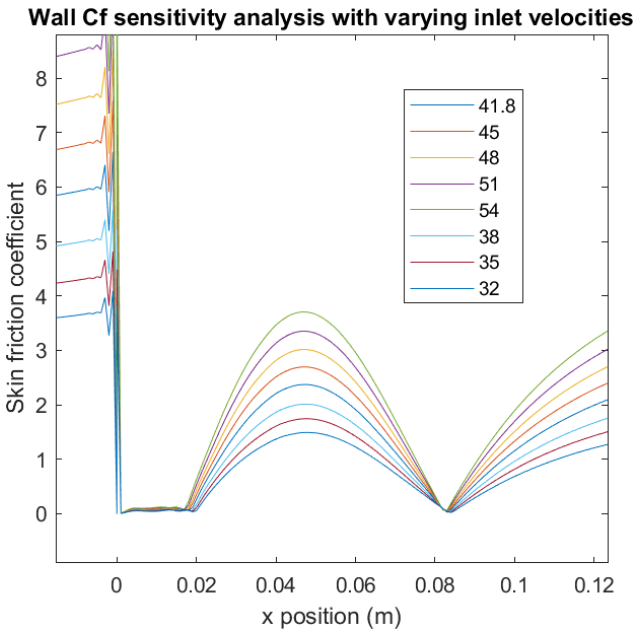

Figure 12: Wall Cf sensitivity analysis with varying inlet velocities Macro view

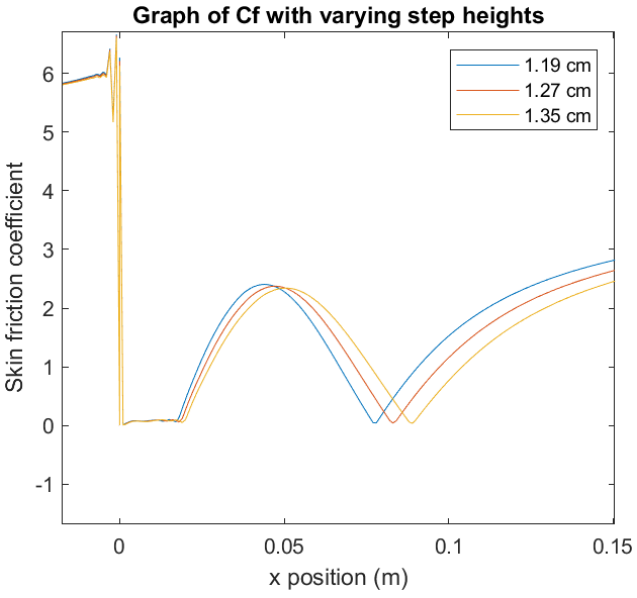

Figure 13: Wall Cf sensitivity analysis with varying step heights

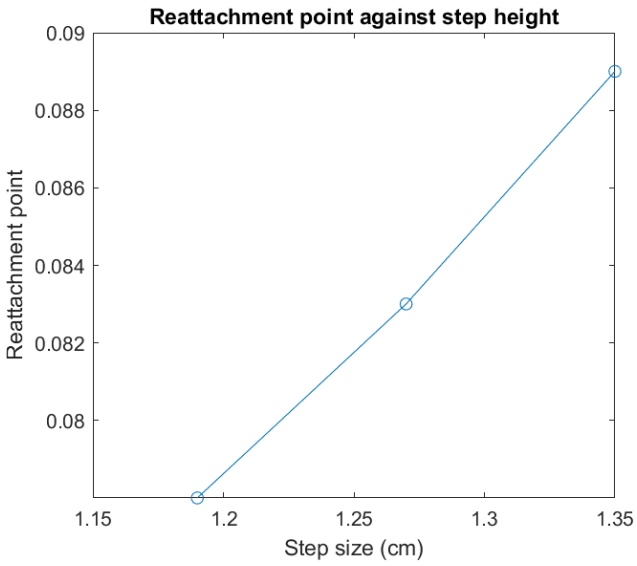

Figure 14: Reattachment point sensitivity analysis varying step height